HYDROLOGICAL PROCESSES
Hydrol. Process. **17**, 3581–3600 (2003)
Published online in Wiley InterScience (www.interscience.wiley.com). DOI: 10.1002/hyp.1348

Year-round observations of the energy and water vapour fluxes above a boreal black spruce forest

M. A. Arain,[1]* T. A. Black,[2] A. G. Barr,[3] T. J. Griffis,[4] K. Morgenstern[2] and Z. Nesic[2]

[1] *McMaster University, Hamilton, Ontario, Canada*
[2] *University of British Columbia, Vancouver, British Columbia, Canada*
[3] *Meteorological Service of Canada, Saskatoon, Saskatchewan, Canada*
[4] *University of Minnesota, St Paul, MN, USA*

Abstract:

Fluxes of energy and water vapour were measured continuously over an ~120-year-old black spruce (*Picea mariana* (Mill.) B.S.P.) forest in northern Saskatchewan, Canada, from 6 May 1999 to 5 May 2001 using the eddy covariance technique as part of the Boreal Ecosystem Research and Monitoring Sites (BERMS) program. These results demonstrate that long-term eddy covariance fluxes can reliably be measured during the harsh boreal winter. Typical daytime bulk surface conductance values were about 5–8 mm s^{-1} during the growing season. Surface conductance sharply declined after midday in response to increasing vapour pressure deficit. The monthly mean values of energy balance components showed that, in spring (March–June), partitioning of available energy flux was mainly in the form of sensible heat, which changed to almost equal proportions of sensible and latent heat in the summer (July–October). In winter (November–February), most of the net radiation was balanced by sensible heat flux. The monthly mean values of net radiation, sensible heat and latent heat flux were about −20 to 20 W m^{-2}, −10 to 25 W m^{-2} and 5 to 10 W m^{-2} respectively in winter. The average mid-day Bowen ratios were approximately 3·5, 1·7 and 5·2 in the spring, summer and winter seasons respectively. The maximum daily evaporation was about 3·5 mm day^{-1} in summer and 0·1–0·25 mm day^{-1} in winter. Over the 2 year period, the accumulated precipitation was 835 mm; this compared with 711 ± 70 mm of evapotranspiration, which showed that more than 85% of water was returned to the atmosphere through evapotranspiration. This study reports the first complete annual cycles of energy and water vapour fluxes at this black spruce site. Since black spruce is the dominant tree species in the North American boreal forest, these results have significance for regional and global energy and water cycles. Copyright © 2003 Crown in the right of Canada. Published by John Wiley & Sons, Ltd.

KEY WORDS evaporation; water vapour flux; sensible heat flux; surface conductance; eddy covariance; black spruce forest

INTRODUCTION

The boreal region has a significant effect on energy, water and carbon budgets of the Northern Hemisphere. For the past two decades this region has been under increased focus of Earth system scientists. It occupies about 21% of the global forested cover, including a 110–180 km wide forest strip from the northwest to southeast of Canada (Schlesinger 1991; Timoney *et al*., 1992; Jarvis *et al*., 1997). In general, conifer species with sparse understory and mosses and lichens covering the forest floor are common in the boreal region. Conifer species are aerodynamically rough and have a low albedo, which allows them to absorb solar radiation and exchange mass and energy with atmosphere efficiently (Jarvis *et al*., 1976; Baldocchi *et al*., 2000). Photosynthesis and transpiration have been observed in boreal conifer species early in the spring, when most of the deciduous species are still dormant (Jarvis *et al*., 1997). In the past, few long-term studies have been conducted to understand the dynamics of energy, water and carbon exchanges over this extensive region.

* Correspondence to: M. A. Arain, School of Geography and Geology, McMaster University, 1280 Main Street West, Hamilton, ON, L8S 4K1, Canada. E-mail: arainm@mcmaster.ca

Received 20 May 2002
Accepted 9 December 2002

In 1993, the Boreal Ecosystem–Atmosphere Study (BOREAS; Sellers *et al*., 1997) was initiated to improve our understanding of the functioning of several key boreal ecosystems, including a black spruce forest in the BOREAS southern study area in central Saskatchewan, Canada (Jarvis *et al*., 1997), referred to as the Southern Old Black Spruce (SOBS). In addition, BOREAS had a black spruce study in the northern study area located in northern Manitoba, Canada (Goulden *et al*., 1998). BOREAS field campaigns greatly improved our understanding of the energy, water and carbon dioxide exchanges of key boreal forest ecosystems. Flux measurements, however, were not made during winter months. Year-round flux measurements are essential to understanding the dynamics of turbulent fluxes and to calculate annual carbon and water budgets accurately. The issue of year-round flux measurements to resolve annual water and carbon budgets is crucial in the North American boreal landscape, which experiences extreme seasonal variation in climatic conditions (Baldocchi *et al*., 2000).

In the spring season of 1999 we initiated year-round observation of momentum, sensible heat, latent heat and carbon dioxide fluxes using the eddy covariance technique at SOBS site as part of the Boreal Ecosystem Research and Monitoring Sites (BERMS) program (Barr *et al*., 2002). The aim of this study was to examine the interactions between a selected boreal ecosystem and the atmosphere throughout the year, quantify seasonal and annual variations in energy, water and carbon exchanges and to relate carbon sink/source strength of this ecosystem to key environmental variables. In this paper we report results of the energy and water vapour flux measurements made over SOBS for the first 2 years of the BERMS experiment from 6 May 1999 to 5 May 2001. The focus of this analysis is to compare, analyse and report the seasonal dynamics of energy and water vapour fluxes for the 2 year period.

MATERIALS AND METHODS

Site description

The SOBS site is located at 53·98 °N, 105·12 °W, about 100 km northeast of Prince Albert, Saskatchewan, Canada. The site was selected in 1993 for BOREAS (Sellers *et al*., 1997). At that time a 25 m tall walk-up scaffold tower was erected to install flux and meteorological instruments above the forest. The site is located near the southern edge of the Canadian boreal forest and is characterized as a typically low-productivity black spruce forest. The site has a slight slope from north to south, which allows runoff of surface water. Topography in the region is predominantly flat, with a few ridges oriented in an east–west direction. The landscape is mostly covered with fens, lakes and forests. The forest consists of pure and mixed stands of black spruce, jack pine (*Pinus banksiana* Lamb), aspen (*Populus tremuloides* Michx.) and tamarack (*Larix laricina* (Du Roi) K. Koch). Black spruce is the dominant vegetation type (57·6% cover area) in the boreal southern study area (Pattey *et al*., 1997). The tower is located in the centre of a lowland black spruce stand with approximately 10% tamarack and occasional jack pine and balsam poplar (*Populus balsamifera* L.), as shown in Figure 1. A dense black spruce stand extends up to 1 km to the north and south, and up to 300 m to the east and west of the tower. In other parts of the fetch, the stand is a mixture of healthy (20–30 cm in diameter), and relatively open and poorly drained patches. The overall fetch is 1200 m in all directions from the tower location (Jarvis *et al*., 1997).

The height of the black spruce stand is 10–12 m, stem diameter at the 1·3 m height is 3–20 cm with a modal diameter of 9–10 cm and stand density is 5900 stems ha^{-1}. The stand is fairly uniform in age (~120 years) because it was regenerated after a fire. Leaf area index (LAI) is highly variable across the site, averaging 4·5 (Chen *et al*., 1997). The live crown of black spruce trees is up to 6 m deep. The exceptionally narrow (<2·5 m in diameter) crowns and densely packed foliage creates significant gaps in the canopy. SOBS has a sparse understory of ~ 1·5 m high shrubs (e.g. *Ledum groenlandicum, Vaccinium vitis-idaea, Salix* spp.), a varied mixed tall herb community (e.g. *Mertensia paniculata, Geum aleppicum, Equisetum sylvaticum*) and occasional dwarf shrubs (e.g. *V. vitis-idaea*). The soil is sandy clay overlain with a 20–30 cm deep hummocky peat layer. The soil surface in wet areas is covered by mosses (e.g. *Hylocomium splendens,*

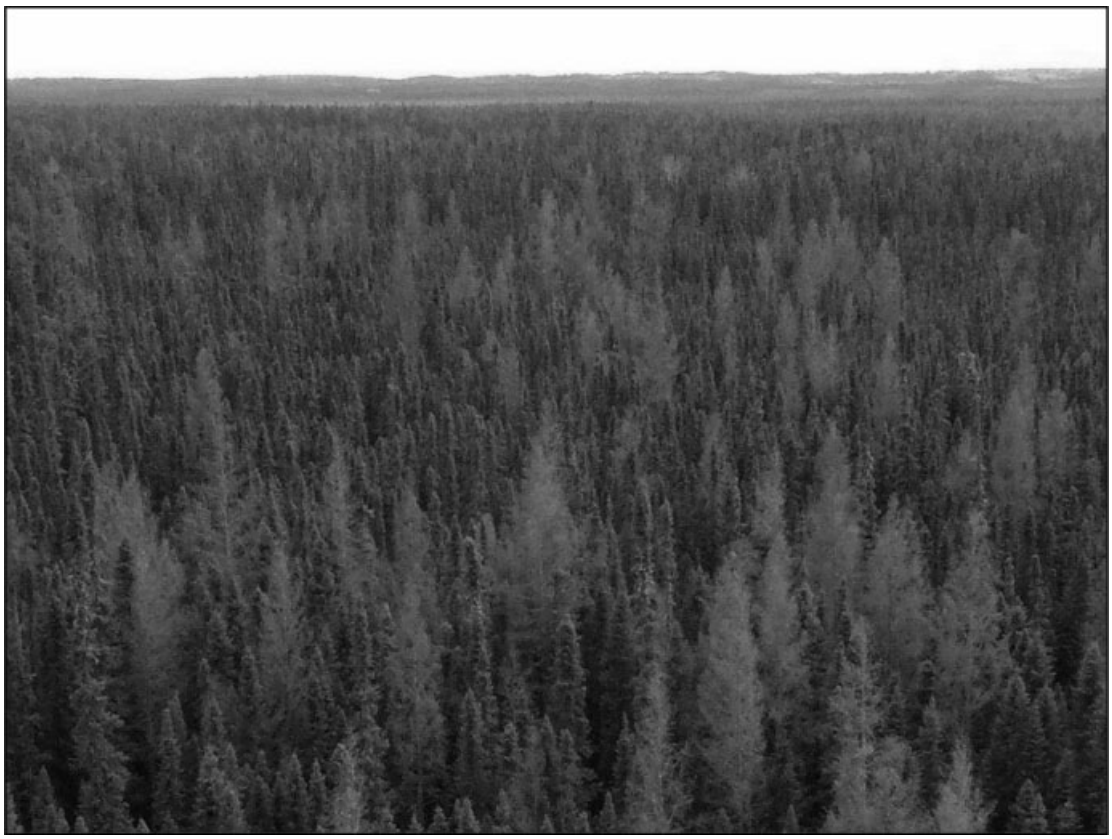

Figure 1. A picture of boreal southern black spruce forest site having about 10% of tamarack and occasional jack pine and balsam poplar. It was taken from the top of the 25 m tower. Light grey species are tamarack and dark species in the background are black spruce

Sphagnum spp.), and lichens (*Cladina* spp.) occupy drier areas. Based on a 30-year climate record, the annual average temperature in the region is 1·0 °C. During the growing season (late April or early May to September), the average air temperature is 13·4 °C. The annual average total precipitation is 400 mm, of which about 40% falls as snow. Measurements show that the water table at the site is often near or at the ground surface. Further site details are given in Sellers *et al*. (1997), Pattey *et al*. (1997) and Jarvis *et al*. (1997).

Eddy covariance flux measurements

As part of the BERMS program, half-hourly above-canopy fluxes of momentum, carbon dioxide (CO_2), sensible heat H and latent heat (LE) were measured from 6 May 1999 to 5 May 2001 using the eddy covariance technique (Baldocchi *et al*., 1996; Chen *et al*., 1999; Aubinet *et al*., 2001). All flux measurements were made above the stand at the 25 m height. Measurements have continued uninterrupted until the writing of this paper; however, measurements after May 2001 are not reported in this paper. Components of the wind vector were measured using a three-dimensional sonic anemometer (model R3, Gill Instruments Ltd, Lymington, UK). Air temperature was calculated from the speed of sound measurements made by the sonic anemometer and were also obtained using two 12·5 μm diameter thermocouples located 0·4 m from the sonic array to provide different estimates of the sensible heat flux. A closed-path infrared gas analyser (IRGA, model 6262, LI-COR Inc., Lincoln, NE, USA) housed in a temperature-controlled box was used to measure CO_2 and water vapour mixing ratios. Air was drawn through a 4·5 m long Dekaron tube (4 mm inner diameter) into the sample cell using a diaphragm pump (model DOA-V191-AA, Gast Inc., Dayton, OH, USA) at 10 l min^{-1}, resulting in

sample cell pressure being 10 kPa less than atmospheric pressure. The short tube length eliminated the need for frequency-response corrections. To prevent condensation, the sampling tube was heated (7–10 °C above ambient temperature) by a voltage (~18 V DC) across a nichrome wire (~20 AWG, ~15 Ω resistance) coiled around the tube and covered by thermal insulation. A 1 μm Teflon filter (Gelman Instruments, Pittsburgh, PA, USA) was positioned just upstream of the IRGA to prevent contamination of the optical chamber. In order to raise the sampled air's temperature to that of the IRGA sample cell, the air was passed through a 3 mm inside diameter, 0·5 m long coiled copper tube, which was sandwiched between aluminium plates, before entering the sample cell. The Dekaron and copper tubes eliminate fluctuations in air temperature of the air stream and simplify the calculation of mixing ratio from mole density (Chen *et al*., 1999). The IRGA was operated in absolute mode with dry nitrogen gas (free of CO_2 and H_2O) continuously passing through the IRGA reference cell at 65 cm^3 min^{-1}. The sampling tube caused a delay time of about 0·8 s in the measurement of the CO_2 and water vapour mixing ratios. The IRGA was calibrated automatically once every 24 h using nitrogen gas for the zero offset check and 360 μmol mol^{-1} CO_2 gas for the CO_2 span check. For the H_2O span check, water vapour mixing ratio values from the IRGA were compared continuously against a humidity sensor (HMP-35C, Vaisala Oyj, Helsinki, Finland) at the same height. Our observations in the field and laboratory environment show that the H_2O zero and span changes are small and follow the pattern of CO_2 zero and span changes. Once a year, we performed a detailed calibration of the IRGA in our laboratory using a dew point generator (model Li-610, Li-COR, Inc. Lincoln, NE, USA). The absolute change of the calibration values for both CO_2 and H_2O spans are usually less than 0·5% for a period of 1 year. All flux data were recorded at 20·833 Hz and raw voltages were saved on a personal computer housed in an instrument hut near the tower. Raw data were also backed up on a Jaz disk (Iomega Corporation, Roy, UT, USA). Fluxes were calculated on-line using software developed at the University of British Columbia. Half-hour fluxes and other meteorological variables were downloaded every midnight by cellular phone to a computer at the University of British Columbia.

Half-hourly CO_2 (and water vapour) fluxes were calculated as the covariance between the vertical wind speed and the CO_2 (and water vapour) mixing ratio (Webb *et al*., 1980; Chen *et al*., 1999). Means over a 0·5 h period were calculated using both block-averaging and linear detrending methods; however, block-averaged value are reported in this paper. Block-averaging removes less low-frequency contribution from data than linear detrending. Our calculations show that the difference between detrended and block-average value was less than 5%. The mean vertical and lateral wind velocity components were rotated to zero to align the vertical velocity measurements normal to the mean wind streamlines following Tanner and Thurtell (1969). Comparison of rotated and non-rotated fluxes showed small difference (<5%) because of the relatively flat topography at the SOBS site. Corrections for pressure broadening and dilution effects of water vapour on CO_2 concentration measurements were applied to the raw voltage data following McDermitt *et al*. (1994) and Chen *et al*. (1999).

Supplementary measurements

Measurements of meteorological variables have been continuous at SOBS since 1994, including air temperature and humidity (HMP-35C), soil temperature (two sets of thermocouples at 2, 5, 10, 20, 50 and 100 cm), soil water content (two sets of soil water content reflectometers) (model 615, Campbell Scientific Inc. (CSI), at 7·5, 22·5, 45 cm), soil heat flux G (four soil heat flux plates at the 10 cm depth for the range of surface situations, CN3, Middleton Instruments, Melbourne, Australia), downwelling and upwelling solar radiation (model CM11 pyranometers, Kipp and Zonen, Delft, Netherlands), downwelling and upwelling longwave radiation (model PIR pyrgeometers, The Eppley Laboratory Inc., Newport, RI, USA) and photosynthetically active radiation (i.e. PAR, model 190SB, Li-COR Inc., Lincoln, NE, USA), wind speed (model 5013 anemometer, R.M. Young Co., Traverse City, MI, USA), barometric pressure, precipitation (Belfort 5915 weighing gauge, with an Alter shield, Belfort Instrument Co., Baltimore, MD, USA) and snow depth (model SR50 Sonic Ranger, CSI). Temperature, humidity, wind speed and wind direction sensors were

installed at the top of tower. The precipitation gauges were mounted at the 3·5 m height on top of the instrument hut to minimize undercatch at high wind speed. The instrument hut is located in a forest clearing approximately one and half tree heights in all directions. Interception of precipitation by the canopy was not measured. The pyranometer and pyrgeometer that measured the downwelling fluxes were mounted in ventilated housings at the top of the flux tower. The ventilators were designed to minimize dew and frost deposition on the radiation sensor domes. The pyranometer and pyrgeometer that measured upwelling fluxes were mounted on a horizontal boom, which extended 4 m to the south of the scaffold tower at 10 m above the forest canopy. Net radiation was calculated from the four components (downwelling and upwelling solar radiations and downwelling and upwelling longwave radiation).

Meteorological data were recorded at 0·5 h intervals on several data loggers (models CR7, CR10 and CR21, CSI).

Data corrections and gap filling and energy balance closure

Errors associated with R_n were in the order of ±5 to 10% because of the influence of the support structure and the accuracy of radiation sensors as specified by their manufacturers. The influence of the support structure was minimized by using the 4 m long boom on which the upwelling pyranometer and pyrgeometer were installed. Most of the meteorological sensors were factory calibrated; however, radiation sensors were calibrated every 2 years. Although the soil water content probes (model 615, CSI) are reported to have a high level of uncertainty for organic soil, our observations and subsequent laboratory tests show that these sensors performed well at SOBS. G was the average of the four soil heat flux plates. It was corrected for heat storage above the flux plates. Measurement of G using only four soil heat flux plates is not adequate at this site. The presence of a thick (20–30 cm) organic layer complicates G measurements because the forest floor insulates the deep soil layers and most of the energy balance is above the ground. This phenomenon is further complicated by local heterogeneity in the forest floor and the presence of a deep moss layer, which has low thermal conductivity. In winter, a thick snow layer insulates the ground. The reader is advised caution while interpreting G results because of the difficulties associated with its measurement at this site. Fortunately, G was usually less then 5% of downwelling solar radiation therefore, even large (~30%) errors in G do not significantly affect the forest's energy balance.

Non-closure of the energy balance is a common feature of eddy covariance measurements above forest ecosystems (Aubinet *et al*., 2001; Wilson *et al*., 2002). Causes of non-closure may include absence of fully developed turbulence at low friction velocity values (i.e. $u_* < 0{\cdot}35$), localized large turbulent structures that cannot be spatially averaged by point measurements, and errors in R_n and G (Lee and Black, 1993). Energy balance closure provides one way of evaluating the performance of turbulent fluxes measured with the eddy covariance system (e.g. H and LE) and the fluxes measured independently (e.g. R_n, G, and canopy heat storage S). The energy balance equation can be written as

$$H + LE = R_n - G - S \tag{1}$$

where $R_n - G - S$ is the available energy flux density. In this study, S was calculated using an empirical relationship that uses the rate of change of air temperature T_a between successive half-hours at the EC sensor height as shown below:

$$S = 13{\cdot}5(\Delta T_a/\Delta t) + 1{\cdot}66 \tag{2}$$

The form of this relationship is similar to that used by Blanken *et al*. (1998) at a nearby aspen ecosystem; however, its constants were adjusted to account for stand biomass at SOBS. Values of S were also calculated using another method, which includes the minor energy balance terms: rate of heat storage in above-ground biomass using bole thermocouples, rate of sensible and latent heat storage in the air column below EC sensors and photosynthetic energy flux. The values of S calculated using this method were in broad agreement with those obtained using the empirical relationship. S was not calculated for the snow pack, and errors associated

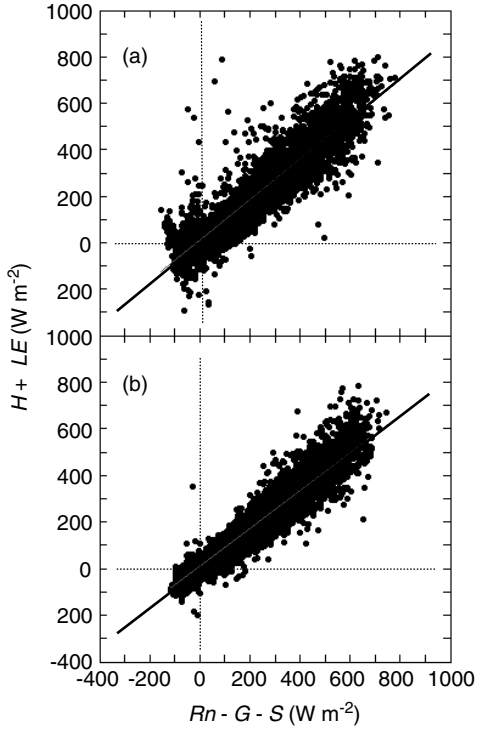

Figure 2. The half-hourly energy balance of the SOBS for (a) 1999–2000 and (b) 2000–01. The sum of sensible heat flux H and latent heat flux (LE) is plotted against net radiation $R_n - G - S$, soil heat flux G and canopy heat storage S (in W m^{-2}). The slopes of the regression lines are 0·86 and 0·81, with intercepts of 8·28 W m^{-2} and 9·20 W m^{-2} for 1999–2000 and 2000–01 respectively. The correlation coefficients r^2 are 0·95 and 0·96 for the first and the second years respectively

Table I. Energy balance closure statistics using half-hourly and daily mean data values

	Half-hourly value				Daily mean value	
	1999–2000 winter	2000–01 winter	1999–2000	2000–01	1999–2000	2000–01
Regression line slope	0·61	0·70	0·86	0·81	0·92	0·87
Regression line intercept (Wm^{-2})	6·78	4·70	8·28	9·20	5·4	4·6
Correlation coefficient r^2	0·74	0·90	0·95	0·96	0·96	0·97

with it may amount to less than 10% during snowfall periods. Figure 2a and b shows the relationship between the half-hourly values of $(H + LE)$ and $(R_n - G - S)$ for 1999–2000 and 2000–01. The slopes of the regression lines are 0·86 and 0·81 and the intercepts are 8·28 W m^{-2} and 9·20 W m^{-2} for 1999–2000 and 2000–01 respectively. Other statistics including the slopes of regression lines, intercepts and correlation coefficients r^2 are given in Table I. In winter (November through to February), half-hourly energy balance closure was not as good as for the entire year (see Table I). Energy balance closure using daily means (24 h) of the components is also commonly reported in the literature (Jarvis *et al.*, 1997). It has the advantage of minimizing the effects of errors in the storage terms because day and night values cancel, but it tends to make closure appear to be better than it really is because there is also cancellation in underestimation of night and daytime EC flux magnitudes. Mean daily closure estimates show regression line slopes of 0·92

and 0·87 with intercepts of 5·4 and 4·6 W m^{-2} for the respective years (Table I). In this study, daytime and night-time H and LE fluxes were corrected to obtain energy balance closure by dividing their magnitudes by the fraction, $f = X[1 - \exp(-u_*/Y)]$ following Blanken *et al.* (1998), where $X = 0{\cdot}93$ and $Y = 0{\cdot}16$ (ms^{-1}). The coefficients X and Y were calculated by plotting $(LE + H)/(R_n - G - S)$ against u_* values. This corrects flux underestimation at values of u_* less then 0·35 m s^{-1}. Low u_* values were most common at night. In order to close energy balance, handle fluxes were increased by 10% ($f = 0{\cdot}90$) at values of u_* greater than 0·35 ms^{-1}. Overall values of H and LE were increased by 3–10%. The terrain at SOBS is flat; therefore, advection (horizontal and vertical) was assumed to average to zero over long periods. Data gaps due to instrument malfunction, power failure and calibration schedule (no more than a few hours) were filled using linear interpolation. Occasional high (>800 W m^{-2}) and low (<−200 W m^{-2}) spikes in turbulent fluxes were removed and filled by linear interpolation. Meteorological data gaps larger than a few half-hours were filled using data from a nearby aspen forest site. Larger data gaps in turbulent fluxes were filled using data from previous days having similar environmental conditions. Overall flux recovery was more than 96%. Out of 4% data loss, 2% was attributed to daily instrument calibrations. Uncertainties in annual evapotranspiration values for both years were estimated to be 10%, which is the sum of measurement uncertainties and data gap filling.

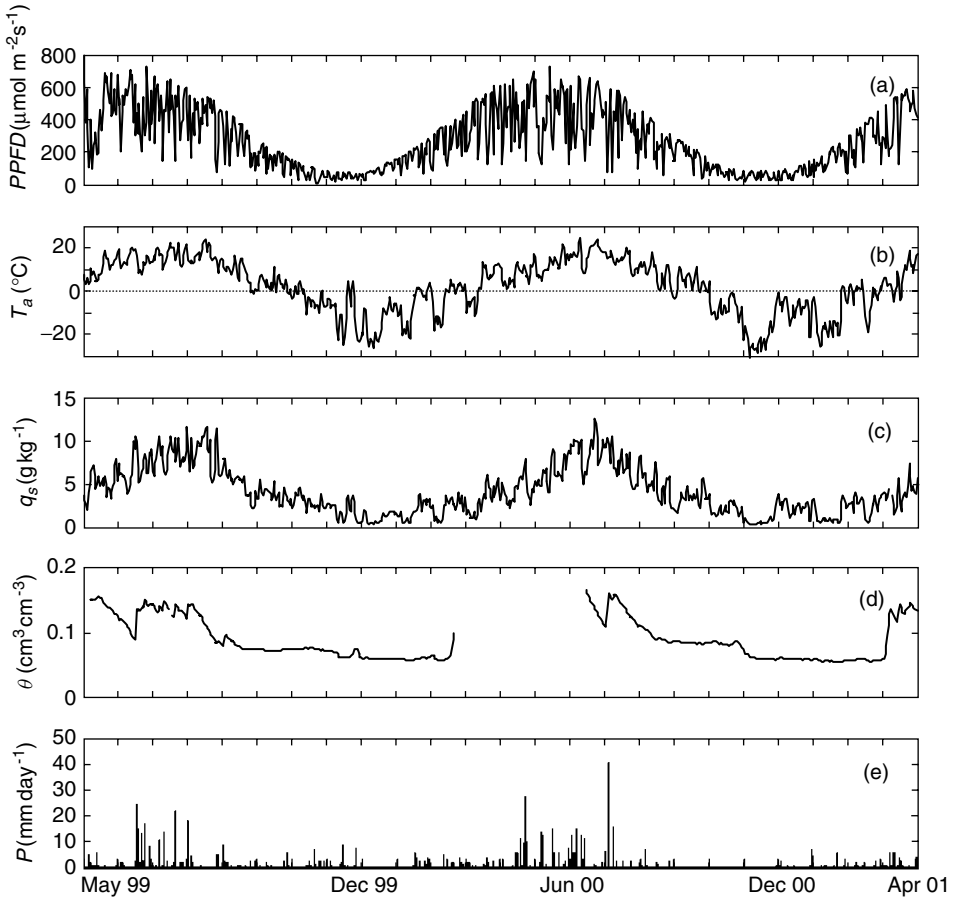

Figure 3. The annual course of the meteorological conditions at the SOBS from 6 May 1999 to 5 May 2001: (a) daily mean photosynthetic photon flux density (PPFD); (b) daily mean air temperature T_a; (c) daily mean specific humidity q_s; (d) daily soil water content θ in upper 7·5 cm soil layer; (e) daily total precipitation P

RESULTS AND DISCUSSION

Climate

The annual courses of daily-mean values of photosynthetic photon flux density (PPFD), T_a, specific humidity q_s, volumetric soil water content θ and precipitation P for 1999–00 and 2000–01 are shown in Figure 3a–e. Maximum daily-mean values of PPFD (720 μmol m^{-2} s^{-1} and 730 μmol m^{-2} s^{-1}), T_a (23·8 °C and 24·1 °C) and q_s (11·5 g kg^{-1} and 12·4 g kg^{-1}) were observed during the summer (in 1999–00 and 2000–01 respectively). Minimum daily-mean values of PPFD (9·1 μmol m^{-2} s^{-1} and 15·8 μmol m^{-2} s^{-1}), T_a (−26·3 °C and −31·3 °C) and q_s (0·27 g kg^{-1} and 0·20 g kg^{-1}) were recorded during the winter (in 1999–00 and 2000–01 respectively). Daily totals of PPFD were modulated by the absence or presence of clouds, particularly in the summer season. There was a slight lag in maximum T_a values compared with maximum values of PPFD. T_a reached its maximum during late July in both years. Minimum values of T_a were recorded in December 1990–2000 and January 2000–01. Total precipitation values during 1999–00 and 2000–01 were 401 mm and 436 mm respectively, which is similar to the 30 year average of 400 mm. Most of the rain fell in the months of June through to August. The time series of precipitation shows that most rainfall events were about 10–15 mm. A maximum daily rainfall of 40·2 mm was recorded on 8 August 2000. Winter and spring precipitation events normally in the form of snow were generally less than 8 mm of water equivalent. Although most of the precipitation fell during summer, soil water content remained high in the root zone (volumetric water content ∼0·5 m^3 m^{-3}) until early August and then decreased rapidly up to the end of September (volumetric water content ∼ 0·25 m^3 m^{-3}). There was no visible indication of water stress in the trees. Soil water content in the upper 7·5 cm soil layer followed precipitation events. Although soil water content values in this layer were lower than in the deeper layers, it never dropped below 0·08 m^3 m^{-3}. The annual average T_a was 2·4 °C and 1·3 °C for 1999–2000 and 2000–01 respectively. The 30 year average value of T_a at this site is 1·0 °C. Fluctuations in daily mean T_a clearly indicated the passage of warm and cold fronts over this site. The effect of a warm front, which caused T_a to rise above zero, thereby causing snow to melt in December 1999, is evident in Figure 3b–d. Synoptic scale variations in T_a were stronger during the winter months, showing ±10 °C change over a few days. Maximum daily-mean soil temperature at the 10 cm depth ranged from 12·1 °C and 13·1 °C during July 1999 and 2000 respectively to −1·8 °C and −4·9 °C during January 2000 and 2001 respectively. Whereas the temperature of the upper 10 cm soil layer followed air temperature, the temperature at the 50 cm depth showed less extreme values, ranging from 1·0 to 9·0 °C.

Albedo

Albedo is a key parameter in soil vegetation atmosphere interaction models (Dickinson, 1992; Kucharik *et al*., 2000). It is used to resolve the radiation and energy balances in these models. It has a significant implication for simulated surface temperature, and hence turbulent fluxes. There is a great deal of uncertainty in the choice of albedo values used in these models (Sellers *et al*., 1997). In the past, most models assumed a winter albedo of about 0·8 (corresponding to fresh snow) for the boreal landscape. Field measurements show that albedo of the boreal conifer forest ecosystems is conservative, and it does not significantly increase during winter when the ground is covered with snow (Betts and Ball, 1997; Baldocchi *et al*., 2000). We calculated the seasonal variations in albedo as a ratio of the daily sum of upwelling shortwave radiation to the daily sum of downwelling shortwave radiation. Because PPFD is critical for carbon exchange modelling, the PPFD albedo was calculated the same way using upwelling and downwelling PPFD values. This method weights the albedo towards the larger midday fluxes (McCaughey *et al*., 1997). Figure 4a and b shows the seasonal course of the two albedos for the two years. During the growing season the mean daily shortwave albedo values were 0·08–0·1, while mean daily PPFD albedo values were 0·03–0·04. These albedo values are low compared with grass and deciduous ecosystems in boreal landscape (Betts and Ball, 1997). Both albedos were relatively high at the start and end of the growing season, with the lowest values being observed in July. Rainfall and overcast conditions significantly decreased albedo on individual days. In October, values

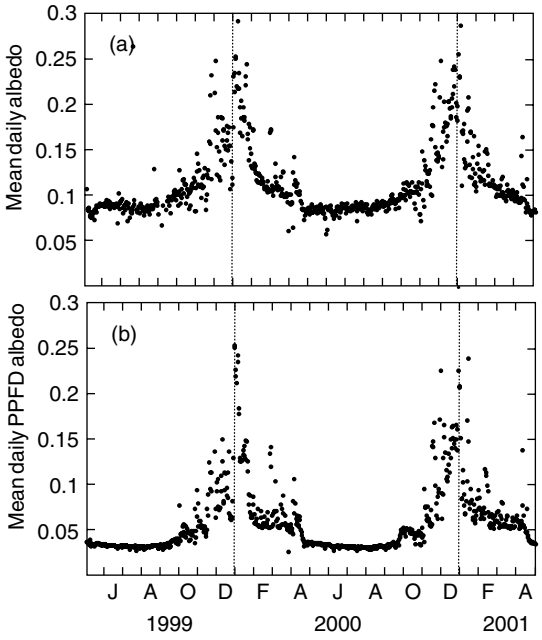

Figure 4. The seasonal courses of the mean daily values of (a) shortwave radiation albedo and (b) photosynthetic photon flux density (PPFD) albedo calculated as the ratios of the daily sums of the upwelling and downmoveing radiation fluxes (W m^{-2} and μmol m^{-2} s^{-1} respectively) from 6 May 1999 to 5 May 2001

of both albedos started to increase, reaching their maxima (approximately 0·25) in December and January. In February and March both the daily shortwave and daily PPFD albedos started to decline again, with typical values of about 0·11–0·13 and 0·05–0·07 respectively. There was a sharp decrease in both albedos after snowmelt in the last week of March. Both years showed a similar course of rise and fall in albedos. These data show that black spruce is a strong absorber of radiation, not only in summer but also in winter months.

Diurnal cycles of energy fluxes in the spring, summer and winter seasons

Figure 5 compares the diurnal cycle of energy fluxes on three typical summer (23–25 August 2000) and winter (21–23 January 2001) days. The 23 and 24 August were partly cloudy and 25 August was a clear summer day. Values of half-hourly Bowen ratio (H/LE) were generally close to 1·6 or so during most summer days. H and LE clearly responded to changes in R_n on those summer days when vapour pressure deficit D was low. The decrease in R_n during afternoon cloudy periods was reflected in H, whereas LE was not significantly affected, indicating that evapotranspiration E was mainly responding to D, as expected in ecosystems with high aerodynamic conductance (McNaughton and Black, 1973). On 24 August values of D were low (<1·2 kPa) throughout the day and there was no effect of D on evaporation. On 23 August and 25 August D was high and evaporation responded strongly to D, particularly on 25 August, which was a sunny and warm day. On this day the LE increased rapidly in the late afternoon hours and then declined near sunset. This shows strong control of D on evaporation rather than bulk surface conductance g_s during these hours (Jarvis *et al.*, 1976, 1997). Increasing D did not cause g_s to drop significantly, thereby reducing E. This has also been observed in other conifer forests with moist soils, such as the Douglas-fir forest at Haney, British Columbia, Canada (McNaughton and Black, 1973). In contrast, conifer forests with less soil water, such as the Douglas-fir forest at the Vancouver Island, British Columbia, and Old Jack Pine in the BOREAS southern study area in Saskatchewan, Canada, showed a drop in E in the afternoon as a result of a strong g_s response to increasing D (Barr *et al.*, 2001; Humphreys *et al.*, 2002). Maximum values of R_n during these summer

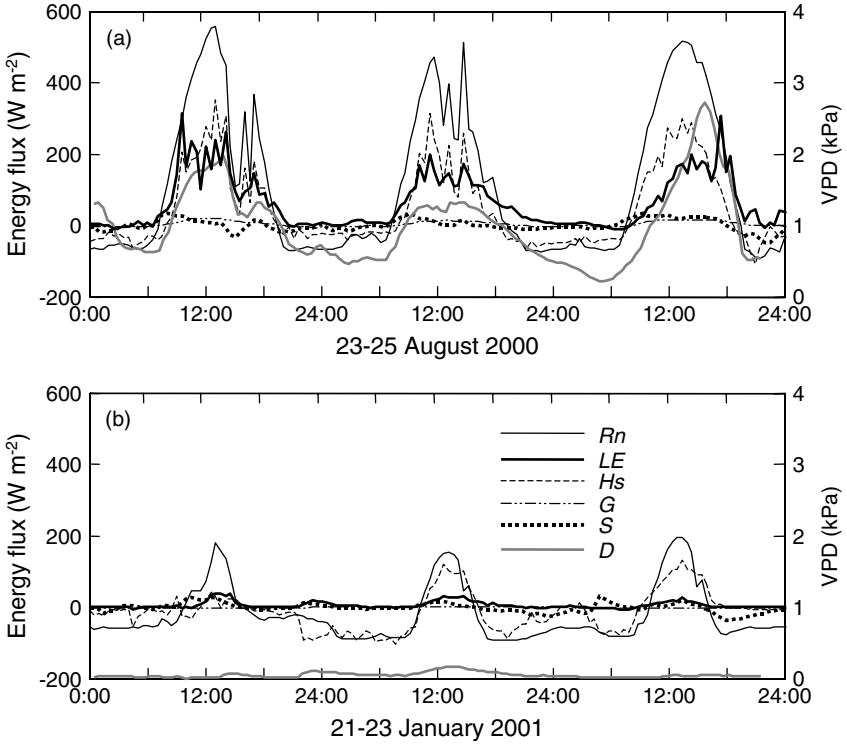

Figure 5. The diurnal courses of net radiation R_n, sensible heat H, latent heat (LE), soil heat flux G and canopy heat storage S (in W m^{-2}) for three typical days in (a) summer, 23–25 August 2000 and (b) winter 21–23 January 2001. Vapour pressure deficit D (kPa) is also shown for both summer and winter days

days were about 500 to 550 W m^{-2}. Afternoon cloudy periods significantly reduced R_n on 23 and 24 August. Maximum values of LE during these 3 days were about 150 to 200 W m^{-2} with occasional half-hour peaks reaching up to 300 W m^{-2}. On warm days H was the dominant turbulent flux, whereas on overcast days the available energy was partitioned equally between H and LE. In winter, when R_n and D were low, most of the available energy was lost in the form of H, e.g. 22 and 23 January. Resolution of winter values of H and LE was almost qualled 1 W m^{-2} (Figure 5b). During daytime hours, LE values were positive mostly because of sublimation of snow. During the night, typically the downward flux of H almost qualled the loss of R_n most of the time.

The contribution of G and S in energy partitioning was small, particularly in the spring and summer seasons. In the winter, however, they were significant part of the energy balance. Values of S showed a distinct early morning peak when heat was being stored in above-ground biomass. This behaviour was observed during both summer and winter days. Maximum values of S were 30 to 33 W m^{-2} during summer and 12 to 31 W m^{-2} during winter. Energy stored in the biomass during the daytime was mostly lost at night. Night-time values of S were -20 to -48 W m^{-2} during summer and -10 to -38 W m^{-2} during winter. During daytime in winter, values of S were similar to those of LE. Values of G, on the other hand, did not show distinct early morning peaks, although they were positive during the day, indicating heat storage, and negative during the night, indicating heat loss. The amplitude of the diurnal cycle of G was small compared with S because of the presence of the thick moss layer on top of the peat soil, both of which have a low thermal conductivity. On summer days, maximum values of G were 14 to 18 W m^{-2} and minimum values were -2 to -5 W m^{-2}. In winter, there was no distinct diurnal pattern in G because of presence of snow on the ground. Winter values of G ranged from -1 to -3 W m^{-2}, indicating a net loss of heat energy.

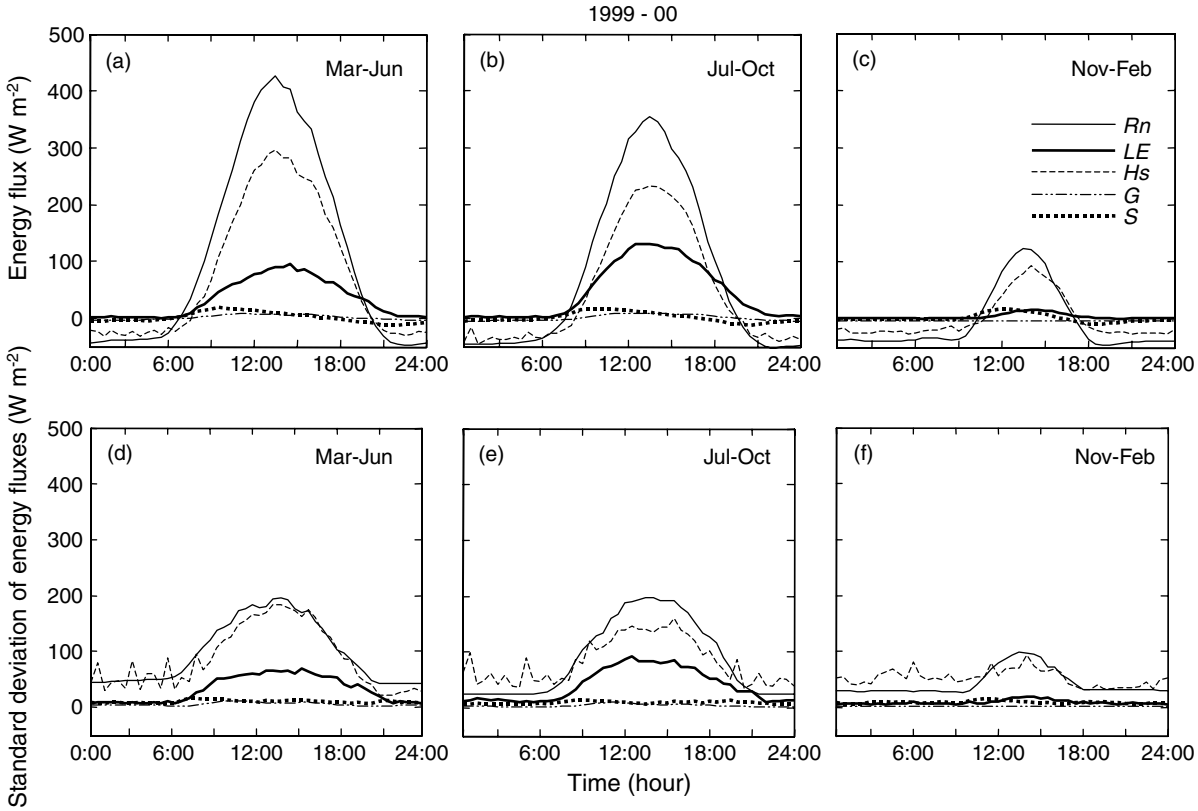

Figure 6. The diurnal course of ensemble averaged net radiation R_n, sensible heat H, latent heat (LE), soil heat flux G and canopy heat storage S (in W m^{-2}) for spring (March to June), summer (July to October) and winter (November to February) of year 1999–2000 in top panels. Standard deviation of energy fluxes are in the bottom panels

Figures 6 and 7 show the mean diurnal courses of R_n, H, LE, G and S and their standard deviations for spring (March–June), summer (July–October) and winter (November–February) in 1999–2000 and 2000–01. These data were calculated by averaging each 0·5 h of the day for the entire period under consideration. In 1999–2000, midday peak values of R_n in spring, summer and winter were 414 W m^{-2}, 347 W m^{-2} and 115 W m^{-2} respectively, whereas in 2000–01 the respective values were 404 W m^{-2}, 365 W m^{-2} and 127 W m^{-2}. In spring and summer, positive R_n values occurred between 06:30–7:30 and 19:30–20:30 CST; in winter, positive R_n values occurred between 9:30 and 17:00 CST. The highest day-to-day variation in R_n occurred in spring and summer afternoons, because of increased cloud cover during that time of year. Sharp reductions in H and LE corresponded to a small decline in R_n. A similar observation was also made by Pattey *et al*. (1997), during the 1994 growing season. In spring, summer and winter, the maximum values of H were 290 W m^{-2}, 228 W m^{-2} and 71 W m^{-2} respectively in 1999–2000, and were 261 W m^{-2}, 204 W m^{-2} and 62 W m^{-2} respectively in 2000–01. In spring, summer and winter, the maximum values of LE were 86 W m^{-2}, 131 W m^{-2} and 14 W m^{-2} respectively in 1999–2000, and were 76 W m^{-2}, 115 W m^{-2} and 12 W m^{-2} respectively in 2000–01. Values of G and S were very small in all three seasons, and their contribution in the overall energy balance was small. Values of S, however, showed an early morning heat gain and a late afternoon heat loss during all three seasons. Midday average Bowen ratio values were 3·4, 1·7 and 5·2 for spring, summer and winter respectively in 1999–2000, and were 3·5, 1·8 and 5·3 respectively in 2000–01. These data show that most of the R_n was partitioned as H. Daily (24 h) Bowen ratio values in 1999–2000 were 2·3, 1·0 and 0·0 for spring, summer and winter seasons respectively, and were 2·3, 1·0

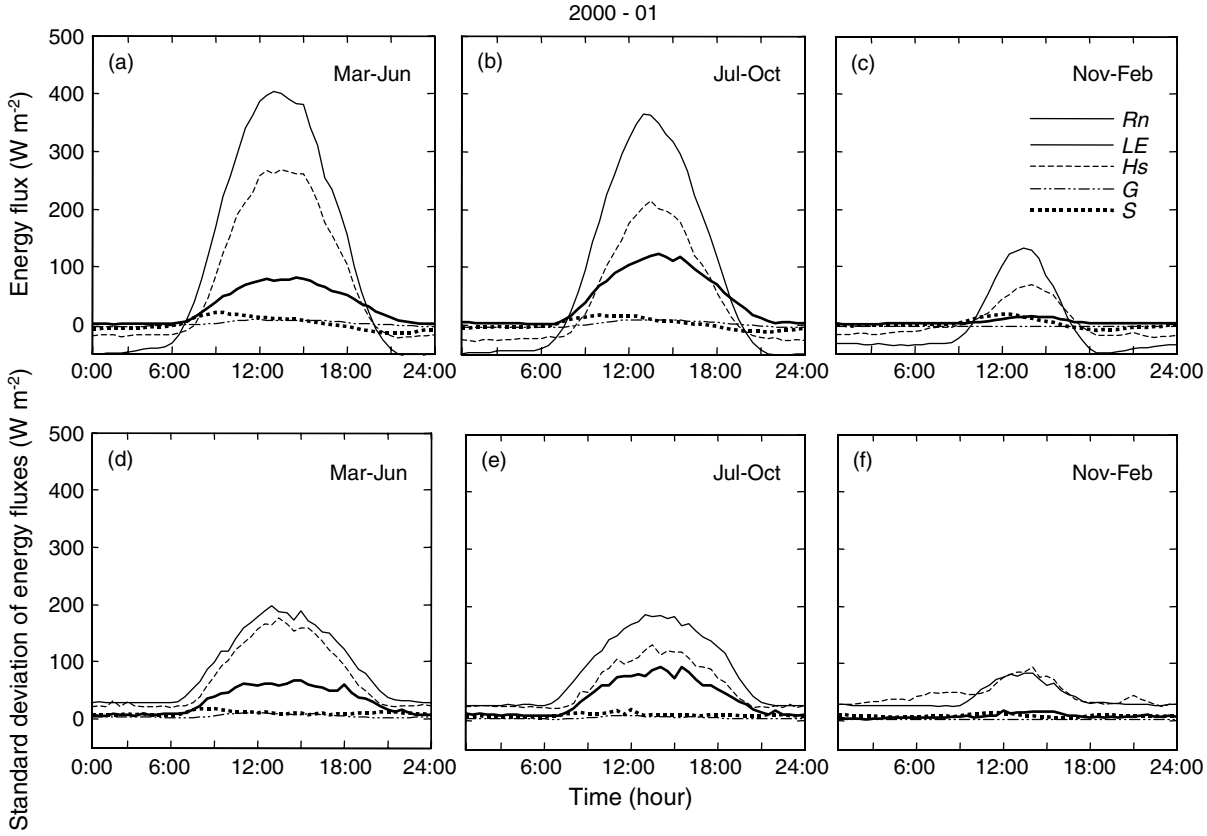

Figure 7. The diurnal course of ensemble averaged net radiation R_n, sensible heat H, latent heat (LE), soil heat flux G and canopy heat storage S (in W m^{-2}) for spring (March to June), summer (July to October) and winter (November to February) of year 2000–01. Standard deviation of energy fluxes are in the bottom panels

and 0·7 respectively in 2000–01. The largest values of midday Bowen ratio were observed in winter, when LE declined because of decreasing surface temperature and available soil water. The Bowen ratio was also high in the spring. Spring and winter Bowen ratio values were similar to those reported for other conifer forests (Jarvis *et al*., 1976; Lafleur, 1997; Baldocchi *et al*., 2000) and semi-desert environments (Sellers *et al*., 1995). During both years, the night-time R_n was approximately -35 W m^{-2} in spring and summer, which was mostly supplied by downward H. In winter, average values of night-time R_n and H were approximately -20 W m^{-2}, while values of LE, G and S were 0–4 W m^{-2}.

Data presented in Figures 6 and 7 shows that H was the dominant turbulent flux throughout the year. Its relative contribution was far more in post snow melt in spring when soil water was frozen in the root zone and was not available to sustain transpiration. These results also show that H closely followed the diurnal pattern of R_n and this relationship was particularly strong in winter. In winter, the rise in H during the day was gradual, particularly in 1999–2000, and the peak value of H occurred about 1 h later than R_n. In spring and summer, LE was positive during the early hours of the day, and even after sunset, whereas the other energy balance components were negative. This phenomenon was also observed in winter, but the overall values of evaporative flux were much smaller. In the spring and winter, peak LE values were observed in early afternoon hours. In the summer, the peak LE was observed around noon, showing changing D and stomatal control on evaporation.

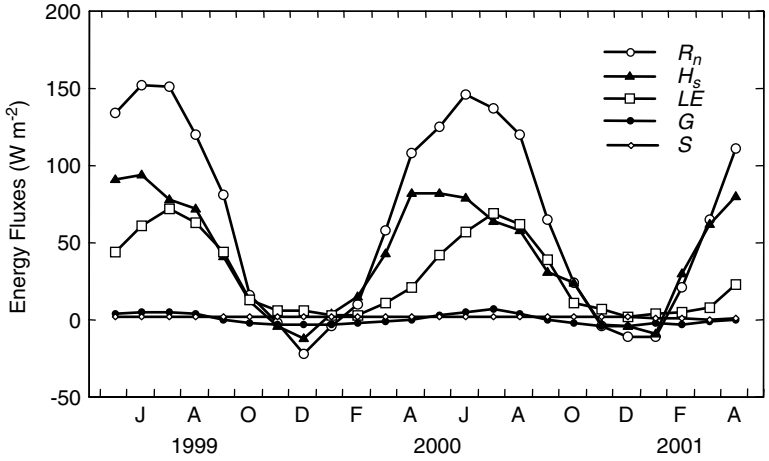

Figure 8. Monthly mean values of net radiation R_n, sensible heat H, latent heat (LE), soil heat flux G and canopy heat storage S (in W m^{-2}) from May 1999 to April 2001

Seasonal cycle of energy fluxes and evaporation

Figure 8 shows the course of the monthly mean values of R_n, H, LE, G and S during the 2 years, calculated by averaging daily (24 h) values. R_n on a monthly basis for this ecosystem ranged from about 150 W m^{-2} in the summer to -10 to 20 W m^{-2} in the winter. More than 90% of R_n was lost as H and LE, whereas the contribution of G and S was very small, which is typical of coniferous forests. There was a small yearly cycle in G ranging from about -5 to 6 W m^{-2}, showing that energy was stored in the soil in summer and released in winter. Maximum values of G were observed in July. As expected, there was no yearly cycle in monthly values of S. Monthly mean H (about 90 W m^{-2}) was much larger than LE (25–65 W m^{-2}) during spring and the early growing season (April through to June), which is also evident in Figures 6 and 7. In June, the ecosystem started to warm gradually and LE started to increase. In July, monthly mean values of LE reached their highest value, approximately 75 W m^{-2}, and were similar to H. These high values of LE were because both soil temperature and D were highest at this time of the year (Jarvis *et al.*, 1997; Baldocchi *et al.*, 2000). Both LE and H gradually declined in September and October because of decreasing solar radiation and soil water content.

In the winter months (November through to February) all energy flux components were small. There was some variability in month-to-month values of R_n as a result of passing winter storms. Most of the available energy was partitioned as H, as indicated earlier. The monthly mean value of H was about -12 to 25 W m^{-2} and LE was approximately 3 to 10 W m^{-2}. There was a strong association between H and R_n, with negative H values occurring in months with the lowest R_n values. LE showed a weak association with R_n and always remained positive throughout winter because of sublimation and occasional increases in evaporation during warm periods. This phenomenon has also been reported for boreal deciduous ecosystems during snow-covered periods (Blanken *et al.*, 1997). Winter R_n and H were highest in the month of February, whereas LE, G and S remained unaffected. Bimonthly values of R_n and ratios of LE and H to R_n over the 2 year period are shown in Table II. This shows that latent heat flux from this forest was conservative and the maximum ratio of LE to R_n ranged from 0·35 to 0·55 during the growing season. This ratio was about 0·94 to 1·0 in winter, except in November–December when R_n was negative and LE was supported by downward H.

The seasonal pattern of the LE, and therefore evaporation, is affected by seasonal changes in air and soil temperatures, radiation, D, θ and LAI (Jarvis *et al.*, 1997; Pattey *et al.*, 1997; Baldocchi *et al.*, 2000). Progression of daily evapotranspiration E through both years is shown in Figure 9. During the summers of 1999 and 2000 the maximum E was about 3–3·5 mm day^{-1} and 0·1–0·25 mm day^{-1} in winter. There

Table II. Net radiation R_n and the ratios of latent heat (LE) and sensible heat H flux to R_n over the 2 year period

Month	R_n	LE/R_n	H/R_n
May–Jun 1999	285	0·36	0·65
Jul–Aug 1999	270	0·49	0·55
Sep–Oct 1999	96	0·57	0·54
Nov–Dec 1999	−25	−0·47	0·68
Jan–Feb 2000	5	1·01	3·4
Mar–Apr 2000	165	0·18	0·75
May–Jun 2000	270	0·36	0·59
Jul–Aug 2000	256	0·51	0·47
Sep–Oct 2000	88	0·55	0·61
Nov–Dec 2000	−16	−0·48	0·47
Jan–Feb 2001	8	0·94	2·41
Mar–Apr 2001	175	0·17	0·81

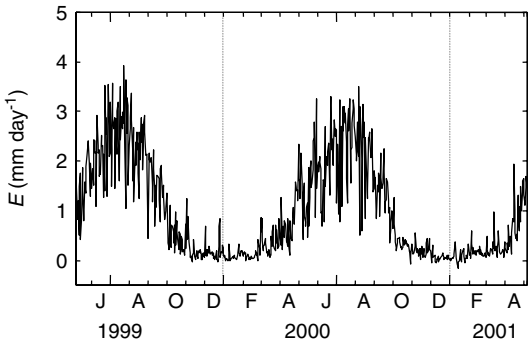

Figure 9. Daily mean of evapotranspiration E (mm day^{-1}) from 6 May 1999 to 5 May 2001

was substantial day-to-day variation depending upon cloudiness, precipitation events or passage of synoptic fronts. Evaporation rates were relatively low in early spring, which had a large proportion of clear days with high atmospheric demand and frozen soil that restricts root uptake of soil water (Halldin *et al.*, 1980). Early spring evaporation was also low because of chilling and frost effects, which affected photosynthesis and stomatal conductance, and hence transpiration (Baldocchi *et al.*, 2000). Evapotranspiration gradually began to rise after snowmelt in late April, reaching a maximum in late June and July, then rapidly decreasing during August and September. In the summer months, high variation in evaporation was a result of changes in cloud cover and D, which are associated with synoptic-scale atmospheric phenomena. In late summer and early winter, the canopy was again exposed to subzero temperatures, which also contributed in decreased evaporation. In autumn, reduction in evaporation was associated with a decrease in soil water and available energy. Available energy values were very low in winter and the air was extremely cold, which reduced D, and hence evaporation. There were occasional 0·5 to 1 mm day^{-1} peaks showing relatively higher evaporation during precipitation event and warmer periods. Annual evapotranspiration from this forest was 366 mm and 345 mm in 1999–00 (365 days) and 2000–01 (366 days) respectively. Cumulative evapotranspiration for the 2 years was 711 ± 70 mm, which was 85% of cumulative precipitation (837 mm; see Figure 10).

Relationship between climatic factors and bulk surface conductance

Bulk surface conductance g_s, defined as the ratio of measured forest *LE* to the difference between the vapour pressure in the stomatal cavities (i.e. the saturation vapour pressure at canopy temperature) and the vapour

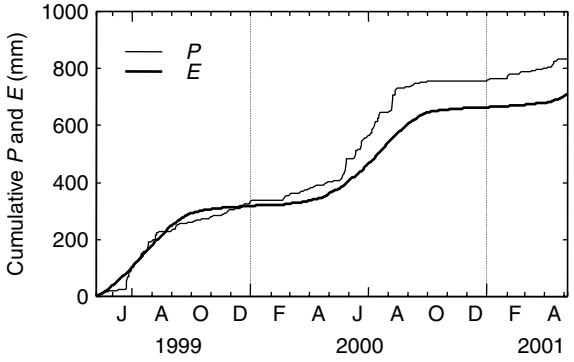

Figure 10. Cumulative precipitation P and evapotranspiration E (mm) from 6 May 1999 to 5 May 2001

pressure at the canopy surface, was calculated using the inverted form of the Penman–Monteith equation (Blanken *et al.*, 1997; Wu *et al.*, 2000):

$$\frac{1}{g_s} = \frac{\rho c_p}{\gamma}\frac{D}{LE} + \left[\left(\frac{s}{\gamma}\right)B_r - 1\right]\frac{1}{g_a} \tag{3}$$

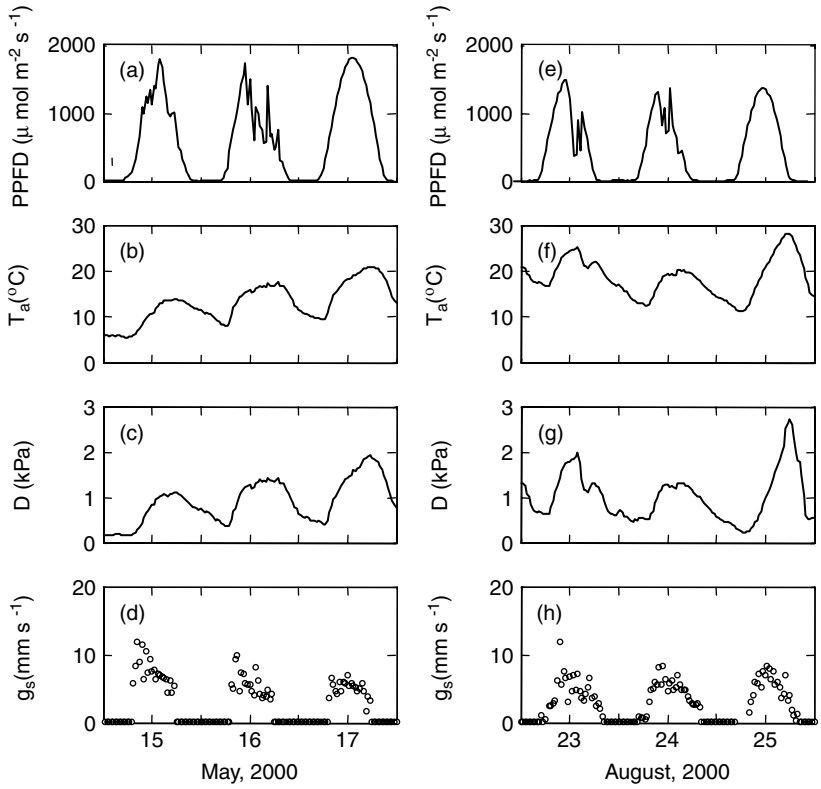

Figure 11. Half-hourly values of photosynthetic photon flux density PPFD (μmol m^{-2} s^{-1}), air temperature T_a (°C), vapour pressure deficit D (kPa) and surface conductance g_s (mm s^{-1}) for three typical days in spring (a–d) and summer (e–h)

where B_r is the Bowen ratio, ρ (kg m^{-3}) is air density, c_p (J kg K^{-1}) is the specific heat of the air, s (kPa K^{-1}) is the change of saturation vapour pressure with temperature, γ (kPa K^{-1}) is the psychrometric constant and g_a (m s^{-1}) is the aerodynamic conductance of the air layer between the canopy and the flux measurement height. g_a was calculated using wind speed and drag coefficient, $g_a = U[k/\ln(z_{ref}/z_{0,M})]^2\Phi_M^{-2}$ following Verseghy *et al*. (1993), where U is the average wind speed above the canopy, k is the von Karmam constant (0·4), z_{ref} is the flux measurement height, $z_{0,M}$ is the roughness length for momentum transfer, and Φ_M is the stability correction factor for momentum. Figure 11 compares the diurnal courses of half-hourly values of g_s and those of climatic factors for 3-day periods early in the growing season and in mid growing season. Typical noontime half-hour values of g_s were 5–9 mm s^{-1} in the growing season, with occasional maxima reaching 11–12 mm s^{-1}. There was a strong correspondence between g_s and those environmental variables. In August, values of T_a and D were the highest of the year. Figure 11d and h shows an early morning rise in g_s, which started to decrease rapidly after midday. Maximum g_s occurred when D and PPFD saturation levels were low early in the morning. As values of PFFD reached a maximum and T_a and hence D began to rise, g_s started to decline rapidly. Since D declined later in the afternoon, the PPFD values were not high enough to support an increase in g_s.

The seasonal courses of daytime mean g_s (9:00 a.m. to 4:00 p.m., PPFD > 200 μmol m^{-2} s^{-1}) for the rain-free periods for 2 years are shown in Figure 12. Estimated values of g_s during early morning hours were not accurate because of the presence of dew on the canopy. In the late afternoon g_s values were erroneous because of low radiation and D. Therefore, g_s values for early morning and late afternoon hours were excluded in Figure 12. Sublimation of snow and the sensitivity of g_s calculations to low D and LE values caused some erroneous values in winter as well (not shown in Figure 12). Daytime mean g_s increased steadily from March through to August and then declined rapidly from September through to October. Typical daytime mean g_s values were approximately 5–10 mm s^{-1}, with maxima reaching 16 mm s^{-1}. The lowest g_s values of 2–3 mm s^{-1} were observed in October for both years. Both years showed a similar pattern of g_s rise with increasing PPFD and T_a in spring and then rapid decline in fall with diminishing available energy. This pattern of g_s rise and fall is in contrast to the course of g_s observed in a nearby boreal deciduous (aspen) forest, which shows a rapid increase in g_s with increasing LAI, reaching a peak in late June and then a gradual decrease from July through to September (Blanken *et al*., 1997). As expected, daytime peak values of g_s for the aspen forest were much higher than for this black spruce forest during the middle of the growing season; however, g_s of the black spruce forest was higher than that of the aspen forest in early spring and late fall. An important characteristic of this conifer ecosystem was the extended growing season with positive g_s values (2–4 mm s^{-1}) in March and October, when the boreal aspen forest (understory and overstory) was virtually leafless. The presence of synoptic weather systems in this region strongly affects g_s because of changes in T_a and D (Blanken *et al*., 1997). g_s drops during cloudy and dry conditions and increases during warm sunny periods. This behaviour of g_s was clearly observed during February 2000, which was a relatively warm

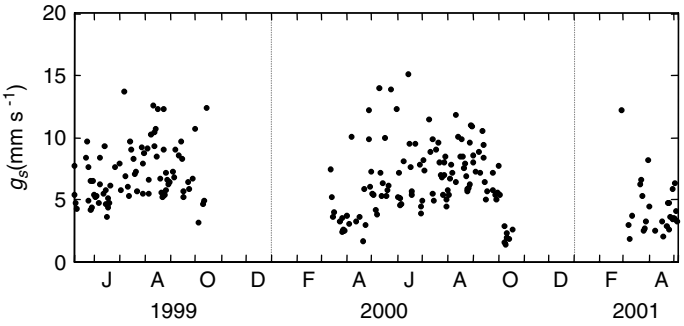

Figure 12. The seasonal course of daytime mean (9:00 a.m. to 4:00 p.m., PPFD > 200 μmol m^{-2} s^{-1} with no precipitation) surface conductance g_s from 6 May 1999 to 5 May 2001

month with daytime mean T_a values reaching $+4\,^{\circ}C$, and during February 2001, which was extremely cold with $T_a < -10\,^{\circ}C$ throughout the month (date not shown in Figure 12). Values of g_s in February 2000 were 3–6 mm s^{-1}, whereas g_s values in February 2001 were mostly erroneous. The relationship between daytime mean g_s (9:00 a.m. to 4:00 p.m., PPFD > 200 μmol m^{-2} s^{-1}) and D for the rain-free periods for the 2 years is shown in Figure 13. The r^2 is 0·21. There is a large scatter in this relationship when values of D are low (<1 kPa). The relationship between g_s and D is strong when D values are high (>1 kPa). This shows that a simple empirical relationship to D is not adequate to estimate g_s in an evapotranspiration model.

The control of daily evaporation by atmospheric and physiological factors can be characterized by the ratio LE/LE_{eq}, which is also known as the Priestley–Taylor α (McNaughton and Jarvis, 1991; Blanken *et al.*, 1997; Baldocchi *et al.*, 2000). The coefficient α provides a simple way to characterize the LE of a stand, rather than using the Penman–Monteith equation. LE_{eq} is the equilibrium latent heat flux, calculated as

$$LE_{eq} = \frac{s}{s+\gamma}(R_n - G - S) \tag{4}$$

Wet ecosystems with an unlimited supply of water have values of $\alpha \geq 1{\cdot}26$, whereas dry ecosystems with lower than potential evaporation rates have values of $\alpha < 1$. Figure 14 shows the seasonal dynamics of daytime mean α (9:00 a.m. to 4:00 p.m., PPFD > 200 μmol m^{-2} s^{-1} with no precipitation) for this black spruce forest during the 2 years. Values of α were low (0·2–0·3) during late winter and early spring, when available energy exceeded the supply of water. α gradually increased, having typical values of 0·5 to 0·7 during the peak of the growing season. Maximum values of α were similar to those reported for low productivity wet and cold boreal ecosystems (Lafleur, 1997; Baldocchi *et al.*, 2000; Barr *et al.*, 2001). These values were much lower than the nearby aspen ecosystem, which showed values of α (>1) typical of well-watered fast-growing crops (Blanken *et al.*, 1997). There was a weak correlation ($r^2 = 0{\cdot}30$) between α and g_s (Figure 15). This relationship was almost linear for g_s values up 6 mm s^{-1}; however, as g_s further increased, there was little increase in α, although there was an ample supply of water in the root zone at this site. Blanken *et al.* (1997) found that, when g_s reached 10 mm s^{-1}, α was about 0·8, whereas in this study α was about 0·7. These results confirm that α of southern boreal black spruce forests is much lower than for aspen and fen ecosystems in the region (Blanken *et al.*, 1997; Barr *et al.*, 2001). Because of lower g_s values transpiration is conservative and a large proportion of the available energy flux is in the form of H. Large H results in a deep planetary boundary layer and considerable entrainment of dry air, which has a negative feedback on stomatal conductance (McNaughton and Spriggs, 1989).

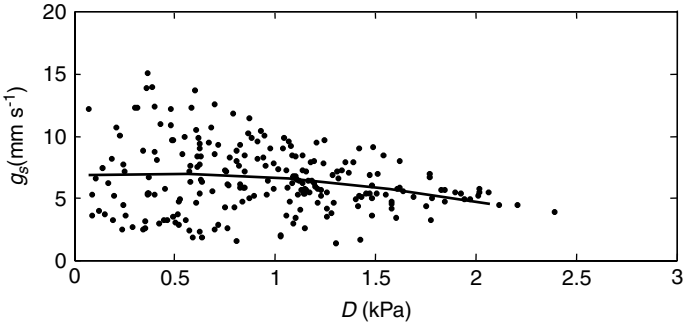

Figure 13. Relationship between daytime mean (9:00 a.m. to 4:00 p.m., PPFD > 200 μmol m^{-2} s^{-1}) values of bulk surface conductance g_s and vapour pressure deficit D for the rain-free periods using data from 6 May 1999 to 5 May 2001. The correlation coefficient r^2 is 0·21. The non-linear curve is fitted by the equation $g_s = -0{\cdot}8165D^2 + 0{\cdot}5765D + 6{\cdot}8794$

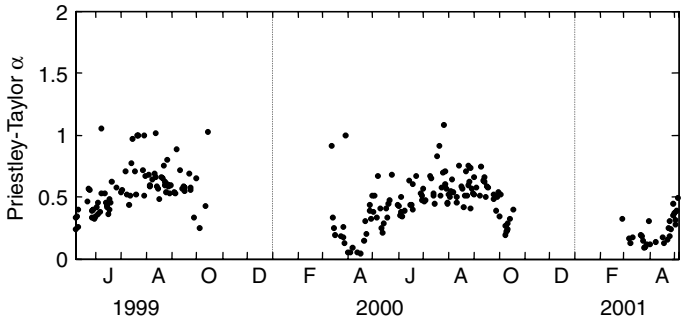

Figure 14. The seasonal course of daytime mean (9:00 a.m. to 4:00 p.m., PPFD > 200 μmol m^{-2} s^{-1} with no precipitation) Priestley–Taylor α from 6 May 1999 to 5 May 2001

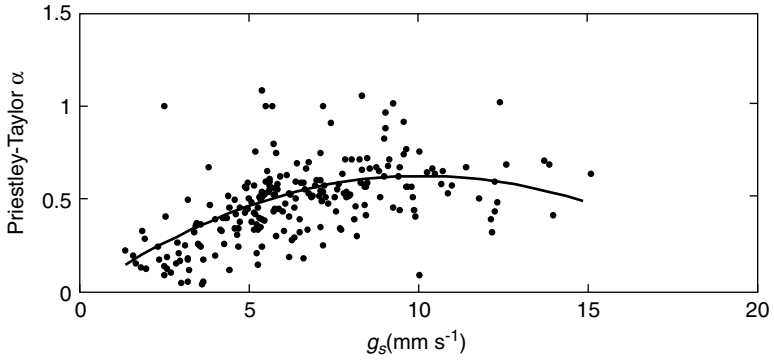

Figure 15. The relationship between daytime mean (9:00 a.m. to 4:00 p.m., PPFD > 200 μmol m^{-2} s^{-1} with no precipitation) Priestley–Taylor α and surface conductance g_s (correlation coefficient $r^2 = 0{\cdot}30$) using data from 6 May 1999 to 5 May 2001. The non-linear curve is fitted by the equation $\alpha = -0{\cdot}0062g_s^2 + 0{\cdot}1265g_s - 0{\cdot}0171$

CONCLUSIONS AND SUMMARY

The results presented in this paper demonstrate that it is possible to collect year-round turbulent flux data, particularly during extremely cold winters. Apart from operational problems, winter flux measurements are difficult to make because of low radiative and turbulent fluxes. Several conclusions can be drawn from this study.

- Monthly mean values of R_n, H, and LE showed that, in spring (April–June), the partitioning of available energy was mainly in the form of H, which changed to almost equal partitioning between H and LE in the summer (July–September). Daily Bowen ratio values were approximately 2·1 and 1·0 in spring and summer respectively.
- In the winter, monthly mean values of R_n, H, and LE were -10 to 20 W m^{-2}, -12 to 25 W m^{-2}, and 3 to 10 W m^{-2} respectively. There was a strong association between H and R_n, with negative H values occurring in the winter months with lowest (negative) R_n values. LE showed a weak association with R_n and always remained positive throughout winter. Daily Bowen ratio values were about 0·0 to 0·7, with midday maximum values reaching 5·2 in winter.
- Maximum daily evapotranspiration in the summer was 3–3·5 mm day^{-1} and in winter was 0·1–0·2 mm day^{-1}, mostly as a result of snow sublimation. Occasional relatively high winter evaporation rates up to 0·5 to 1 mm day^{-1} were observed during the passage of warm synoptic weather fronts.

- Total evapotranspiration for the 2 years was 711 ± 70 mm and total precipitation was 837 mm, indicating that 85% of precipitation was lost in the form of evapotranspiration.
- Daytime mean g_s increased steadily during the growing season and then declined rapidly in fall, with typical maximum values of approximately 5–10 mm s^{-1}. During both years, g_s showed a similar pattern of rise with increasing PPFD and T_a and then rapid decline with decrease in available energy.

ACKNOWLEDGEMENTS

Funding for this study was provided by the Natural Sciences and Engineering Research Council of Canada, Canadian Foundation of Innovation, Ontario Innovation Trust, Canadian Foundation for Climate and Atmospheric Sciences, Meteorological Service of Canada, Canadian Forest Service, Parks Canada, Program of Energy Research and Development (PERD), Canada, and National Aeronautical and Space Administration (NASA), USA. We gratefully acknowledge the advice and assistance from Hok Woo and Jim Smith. We are very grateful to anonymous reviewers for their constructive comments, which significantly improved the quality of this paper.

REFERENCES

Aubinet M, Chermanne B, Vandenhaute M, Longdoz B, Yernaux M, Laitat E. 2001. Long-term carbon dioxide exchange above a mixed forest in the Belgian Ardennes. *Agricultural and Forest Meteorology* **108**: 293–315.

Baldocchi DD, Valentini R, Oechel W, Dahlman R. 1996. Strategies for measuring and modelling carbon dioxide and water vapour fluxes over terrestrial ecosystems. *Global Change Biology* **2**(3): 159–168.

Baldocchi D, Kelliher FM, Black TA, Jarvis PJ. 2000. Climate and vegetation controls on boreal zone energy exchange. *Global Change Biology* **6**(1): 69–83.

Barr AG, Bett AK, Black TA, McCaughey JH, Smith CD. 2001. Intercomparison of BOREAS northern and southern study area surface fluxes in 1994. *Journal of Geophysical Research* **106**: 33 543–33 550.

Barr AG, Griffis TJ, Black TA, Lee X, Staebler RM, Fuentes JD, Chen Z, Morgenstern K. 2002. Comapring the carbon budgets of boreal and temperate deciduous forest stands.*Canadian Journal of Forest Research* **32**: 813–822.

Betts AK, Ball JH. 1997. Albedo over the boreal forest. *Journal of Geophysical Research* **102**: 28 901–28 909.

Blanken PD, Black TA, Yang PC, den Hartog G, Neumann HH, Nesic Z, Novak MD, Staebler R, Lee X. 1997. Energy balance and surface conductance of a boreal aspen forest: partitioning overstory and understory components. *Journal of Geophysical Research* **102**: 28 915–28 927.

Blanken PD, Black TA, Neumann HH, den Hartog G, Yang PC, Nesic Z, Staebler R, Chen W, Novak MD. 1998. Turbulent flux measurements above and below the overstory of a boreal aspen forest. *Boundary-Layer Meteorology* **89**: 109–140.

Chen JM, Rich PM, Gower ST, Norman JM, Plummer S. 1997. Leaf area index of boreal forests: theory, techniques, and measurements. *Journal of Geophysical Research* **102**: 29 429–29 443.

Chen WJ, Black TA, Yang PC, Barr AG, Neumann HH, Nesic Z, Blanken PD, Novak MD, Eley J, Ketler RJ, Cuencas R. 1999. Effects of climate variability on the annual carbon sequestration by a boreal aspen forest. *Global Change Biology* **5**: 41–53.

Dickinson RE. 1992. Land surface. In *Climate System Modelling*, Trenberth KE (ed.). Cambridge University Press: 35–65.

Goulden ML, Wofsy SC, Harden JW, Trumbore SE, Crill PM, Gower ST, Fries T, Daube BC, Fan SM, Sutton DJ, Bazzaz A, Munger JW. 1998. Sensitivity of boreal forest carbon balance to soil thaw. *Science* **279**: 214–217.

Halldin S, Grip H, Jansson PE, Lindgren A. 1980. Micrometeorology and hydrology of pine forest ecosystems. II. Theory and models. In *Structure and Function of Northern Coniferous Forests—An Ecosystem Study*, Persson T (ed.). *Ecological Bulletin (Stockholm)* **32**: 463–503. .

Humphreys ER, Black TA, Ethier GJ, Drewitt GB, Spittlehouse DL, Jork E-M, Nesic Z, Livingston NJ. 2003. Annual and seasonal variability of sensible and latent heat fluxes above a coastal Douglas-fir forest, British Columbia, Canada. *Agricultural and Forest Meteorology* **115**: 109–125.

Kucharik CJ, Foley JA, Delire C, Fisher VA, Coe MT, Lenters JD, Young-Molling C, Ramankutty N. 2000. Testing the performance of a dynamic global ecosystem model: water balance, carbon balance, and vegetation structure. *Global Biogeochemical Cycles* **14**(3): 795–825.

Jarvis PG, James GB, Landsberg JJ. 1976. Coniferous forest. In *Vegetation and the Atmosphere*, vol. 2, Monteith JL (ed.). Academic Press: London; 171–240.

Jarvis PG, Massheder JM, Hale SE, Moncrieff JB, Rayment M, Scott SL. 1997. Seasonal variation of carbon dioxide, water and energy exchanges of a boreal black spruce forest. *Journal of Geophysical Research* **102**: 28 953–28 966.

Lafleur P. 1997. Energy balance and evapotranspiration from a subarctic forest. *Agricultural and Forest Meteorology* **58**: 163–175.

Lee X, Black TA. 1993. Atmospheric turbulence within and above a Douglas-fir stand. Part I: statistical properties of the velocity field. *Boundary-Layer Meteorology* **84**: 383–398.

McCaughey JH, Lafleur PM, Joiner DW, Bartlet PA, Costello AM, Jelinski DE, Ryan MG. 1997. Magnitudes and seasonal patterns of energy, water and carbon exchanges at a boreal young jack pine forest in the BOREAS northern study area. *Journal of Geophysical Research* **102**: 28 997–29 007.

McDermitt DK, Welles JM, Eckles RD. 1994. *Effects of temperature, pressure and water vapour on gas phase infrared absorption by CO_2*. Application Note # 116, Li-COR, Lincoln, NB, USA.

McNaughton KG, Black TA. 1973. A study of evapotranspiration from Douglas fir forest using the energy balance approach. *Water Resources Research* **9**: 1579–1590.

McNaughton KG, Jarvis PG. 1991. Effects of spatial scale on stomatal control of transpiration. *Agricultural and Forest Meteorology* **54**: 279–302.

McNaughton KG, Spriggs TW. 1989. An evaluation of the Priestley and Taylor equation and the complementary relationship using results from a mixed-layer model of the convective boundary layer. In *Estimation of Areal Evapotranspiration*, Black TA, Spittlehouse DL, Novak MD, Price DT (eds). IAHS Publication no. 177. IAHS Press: Wallingford; 89–104.

Pattey E, Desjardin RL, St-Amour G. 1997. Mass and energy exchange over a black spruce forest during key periods of BOREAS 1994. *Journal of Geophysical Research* **102**: 28 967–28 975.

Schlesinger WH. 1991. *Biogeochemistry: An Analysis of Global Change*. Academic Press: San Diego, CA.

Sellers PJ, Hall FG, Margolis H, Kelly RD, Baldocchi DD, *et al*. 1995. The Boreal Ecosystem–Atmosphere Study (BOREAS): an overview and early results from the 1994 field year. *Bulletin of the American Meteorological Society* **76**: 1549–1577 .

Sellers PJ, Hall FG, Kelly RD, Black TA, Baldocchi DD, *et al*. 1997. BOREAS in 1997: experiment overview, scientific results, and future directions. *Journal of Geophysical Research* **102**: 28 731–28 769 .

Tanner CB, Thurtell GW. 1969. *Anemoclinometer measurements of Reynolds stress and heat transport in the atmospheric boundary layer*. Research and Development Technical Report ECOM66-G22F, University of Wisconsin, Madison, WI, USA.

Timoney KP, Roi La GH, Zoltai SC, Robinson AL. 1992. The high subarctic forest tundra region on northwestern Canada: position, width and vegetation gradients in relation to climate. *Arctic* **45**: 1–9.

Verseghy DL, McFarlane NA, Lazare M. 1993. CLASS—a Canadian land surface scheme for GCMs, II. Vegetation model and coupled runs. *International Journal of Climatology* **13**: 347–370.

, Webb EK, Pearman GI, Leunning R. 1980. Correction of flux measurements for density effects due to heat and water vapour transfer. *Quarterly Journal of the Royal Meteorological Society* **106**: 85–100.

Wilson K, Goldstein A, Falge E, Aubinet M, Baldocchi D, *et al*. 2002. Energy balance closure at FLUXNET sites. *Agricultural and Forest Meteorology* **113**: 223–243. .

Wu A, Black TA, Verseghy DL, Blanken PD, Novak MD, Chen W, Yang PC. 2000. A comparison of parameterization of surface conductance of aspen and Douglas-fir forest for CLASS. *Atmosphere–Ocean* **38**: 81–112.

